On the Origin of Radio Emission in the X-Ray States of XTE J1650-500 during the 2001-2002 Outburst

Corbel, S.; Fender, R.P.; Tomsick, J.A.; Tzioumis, A.K.; Tingay, S.

DOI
10.1086/425650

Publication date
2004

Published in
Astrophysical Journal

The Astrophysical Journal, 617:1272–1283, 2004 December 20

ON THE ORIGIN OF RADIO EMISSION IN THE X-RAY STATES OF XTE J1650−500 DURING THE 2001–2002 OUTBURST

S. Corbel,[1] R. P. Fender,[2] J. A. Tomsick,[3] A. K. Tzioumis,[4] and S. Tingay[5]

Received 2004 June 11; accepted 2004 August 13

ABSTRACT

We report on simultaneous radio and X-ray observations of the black hole candidate XTE J1650−500 during the course of its 2001–2002 outburst. The scheduling of the observations allowed us to sample the properties of XTE J1650−500 in different X-ray spectral states, namely, the hard state, the steep power-law state, and the thermal dominant state, according to the recent spectral classification of McClintock & Remillard. The hard state is consistent with a compact jet dominating the spectral energy distribution at radio frequencies; however, the current data suggest that its contribution as direct synchrotron emission at higher energies may not be significant. In that case, XTE J1650−500 may be dominated by Compton processes (either inverse Comptonization of thermal disk photons and/or synchrotron self-Compton radiation from the base of the compact jet) in the X-ray regime. We surprisingly detect a faint level of radio emission in the thermal dominant state that may be consistent with the emission of previously ejected material interacting with the interstellar medium, similar (but on a smaller angular scale) to what was observed in XTE J1550−564 by Corbel and coworkers. Based on the properties of radio emission in the steep power-law state of XTE J1650−500 and taking into account the behavior of other black hole candidates (namely, GX 339−4, XTE J1550−564, and XTE J1859+226) while in the intermediate and steep power-law states, we are able to present a general pattern of behavior for the origin of radio emission in these two states that could be important for understanding the accretion-ejection coupling very close to the black hole event horizon.

Subject headings: accretion, accretion disks — black hole physics — ISM: jets and outflows — radio continuum: stars — stars: individual (GX 339−4, XTE J1550−564, XTE J1650−500, XTE J1859+226)

1. INTRODUCTION

XTE J1650−500 is a soft X-ray transient discovered on 2001 September 5 (MJD 52,157; Remillard 2001) by the All-Sky Monitor on board the *Rossi X-Ray Timing Explorer* (*RXTE* ASM). On the next day, pointed *RXTE* PCA (Proportional Counter Array) observations confirmed the ASM detection of XTE J1650−500 with an X-ray spectrum typical of a black hole candidate (BHC) in the hard state (HS) (Markwardt et al. 2001). This was confirmed by further analysis of the power density spectra (Revnivtsev & Sunyaev 2001; Wijnands et al. 2001). During the course of the outburst, XTE J1650−500 went into all the canonical X-ray spectral states (Rossi et al. 2004) that are typical of the population of BHCs (Belloni 2004; McClintock & Remillard 2004). High-frequency quasi-periodic oscillations (QPOs) have been reported by Homan et al. (2003). The possible detection of a broad iron Kα emission (e.g., Miller et al. 2002) may suggest that XTE J1650−500 is a maximal Kerr black hole. In addition, short ($\sim$100 s) X-ray flares and long-timescale oscillations have been reported by Tomsick et al. (2003b) during the decay to quiescence.

The optical counterpart was discovered by Castro-Tirado et al. (2001) with the 0.6 m optical telescope at Lake Tekapo, New Zealand. The identification was later confirmed by Groot et al. (2001) and Augusteijn et al. (2001). The radio counterpart was discovered with the Australia Telescope Compact Array (ATCA) located in Narrabri, Australia (Groot et al. 2001). Further optical observations of XTE J1650−500 in quiescence with the 6.5 m Magellan telescope and the 8 m Very Large Telescope revealed the orbital parameters of this system (Orosz et al. 2004). The companion star is of spectral type K3 V–K5 V, and the orbital period of the system is 0.3205 days. The mass function of $2.73 \pm 0.56\ M_{\odot}$ and the lower limit on the inclination angle of $50^{\circ} \pm 3^{\circ}$ (in contradiction to what was originally proposed by Sanchez-Fernandez et al. [2002]) give an upper limit of $7.3\ M_{\odot}$ for the mass of the compact object. The primary in the XTE J1650−500 system is likely a black hole, and in fact, the existing data suggest that it could be a black hole with a mass of only $4\ M_{\odot}$ (Orosz et al. 2004).

In this paper we report on X-ray and radio observations of XTE J1650−500 spread over the entire outburst. In § 2 we describe the observations and the outburst evolution. We then discuss the properties of the radio emission from XTE J1650−500 in each of the states covered by our observations, including the HS, the steep power-law (SPL) state (we also discuss the nature of the intermediate state [IS]), the thermal dominant (TD) state, and the state transitions. Our conclusions are summarized in § 4. Our X-ray state definitions are nearly the same as the new definitions described in the review by McClintock & Remillard (2004). In this work we follow McClintock & Remillard (2004) by using the names HS and TD state rather than the previous names (low-hard state and high-soft state, respectively) to designate the two best-known X-ray states. The

[1] Université Paris 7, Denis Diderot, and Service d'Astrophysique, UMR AIM, CEA Saclay, F-91191 Gif-sur-Yvette, France.
[2] Astronomical Institute 'Anton Pannekoek' and Center for High Energy Astrophysics, University of Amsterdam, Kruislaan 403, 1098 SJ Amsterdam, Netherlands.
[3] Center for Astrophysics and Space Sciences, University of California at San Diego, MS 04-24, La Jolla, CA 92093.
[4] Australia Telescope National Facility, CSIRO, P.O. Box 76, Epping, NSW 1710, Australia.
[5] Center for Astrophysics and Supercomputing, Swinburne University of Technology, Mail Number 31, P.O. Box 218, Hawthorn, VIC 3122, Australia.

TABLE 1
Observing Log and Results

Parameter	Observation							
	1	2	3	4	5	6	7	8
Date (MJD)[a]	52159.94	52160.81	52177.01	52187.67	52195.85	52204.25	52241.52	52247.63
Calendar date	2001 Sep 7	2001 Sep 8	2001 Sep 24	2001 Oct 5	2001 Oct 13	2001 Oct 21	2001 Nov 27	2001 Dec 4
Time on source (hr)[b]	0.66, 1.09	1.16, 0.99	1.29	4.10	3.75	1.80	6.56	2.73
Array configuration	6B	6B	0.750D	EW352	EW352	EW352	6D	6D
Flux density (mJy):								
1384 MHz	2.7 ± 0.3	4.08 ± 0.20	...	...	...	...	...	...
2496 MHz	2.3 ± 0.2	5.30 ± 0.15	...	...	...	...	...	...
4800 MHz	...	5.28 ± 0.10	0.83 ± 0.10	<0.21	1.29 ± 0.07	0.78 ± 0.10	1.21 ± 0.06	0.75 ± 0.10
8640 MHz	...	4.48 ± 0.10	0.77 ± 0.10	<0.18	0.91 ± 0.10	0.34 ± 0.09	1.15 ± 0.06	<0.30
Spectral index	−0.27 ± 0.31	−0.29 ± 0.04[c]	−0.13 ± 0.86	...	−0.59 ± 0.56	−1.41 ± 1.36	−0.09 ± 0.18	<−1.3
X-ray state	HS	HS	SPL	SPL	TD	TD	HS	HS
X-ray flux[d]	10.40 ± 0.10	10.96 ± 0.11	10.47 ± 0.10	10.31 ± 0.10	10.04 ± 0.10	7.25 ± 0.07	1.75 ± 0.08	1.13 ± 0.06

Note.—Upper limits are given at the 3 σ confidence level.
[a] Radio observation midpoint.
[b] The first number is for the observations at 1384 and 2496 MHz (if noted); otherwise, it is related to the observations at 4800 and 8640 MHz.
[c] Spectral index obtained if we fit the radio spectrum with a power law and thermal free-free absorption. If we use the two higher frequencies, a spectral index of -0.28 ± 0.14 is deduced.
[d] Unabsorbed 2–11 keV flux in units of 10^{-9} ergs s^{-1} cm^{-2}.

difference between our definitions and those of McClintock & Remillard (2004) concerns the intermediate and very high states, which could possibly be various instances of the same state (e.g., Homan et al. 2001; Belloni 2004). McClintock & Remillard (2004) divided these two flavors of the intermediate/very high state as follows: First is the soft (i.e., photon index >2.4) flavor, which has a steep power-law spectrum and was therefore called the SPL state. In the SPL state, low- and high-frequency QPOs are usually detected. The interpretation of the IS in McClintock & Remillard (2004) is more ambiguous, as it is defined in terms of combinations of the other spectral states. In this work we define the IS as having properties between the HS and SPL state, so that the IS is essentially a hard flavor of the intermediate/very high state mentioned previously.

2. OBSERVATIONS AND OUTBURST OVERVIEW

2.1. *Radio Observations*

During the X-ray outburst of XTE J1650−500, we conducted eight continuum radio observations with ATCA, located in Narrabri, New South Wales, Australia. The ATCA synthesis telescope is an east-west array consisting of six 22 m antennas. The ATCA uses orthogonal polarized feeds and records full Stokes parameters. We carried out observations mostly at 4800 MHz (6.3 cm) and 8640 MHz (3.5 cm) with the exception of the first two observations, for which we also made measurements at 1384 MHz (21.7 cm) and 2496 MHz (12.0 cm). For the first observation, because of the large uncertainty in the X-ray position at that time, the radio counterpart of XTE J1650−500 was outside the primary beam of the telescope at 4800 and 8640 MHz. We performed observations in various array configurations: 6B (baselines ranging from 214 to 5969 m), 6D (77–5878 m), 0.750D (31–4469 m), and EW352 (31–4438 m), in order of decreasing spatial resolution. An additional observation (6A configuration) was conducted on 2003 December 21 while XTE J1650−500 was in quiescence. We did not detect XTE J1650−500 with a 3 σ upper limit of 0.3 mJy at 4800 and 8640 MHz.

The amplitude and bandpass calibrator was PKS 1934−638, and the antenna's gain and phase calibration, as well as the polarization leakage, were derived from regular observations of the nearby (less than a degree away) calibrator PMN 1646−50. The editing, calibration, Fourier transformation, deconvolution, and image analysis were performed using the MIRIAD software package (Sault & Killeen 1998). An observing log, as well as the ATCA flux densities of XTE J1650−500, can be found in Table 1. The dates of our ATCA observations are indicated in Figures 1 and 2 in order to illustrate how they are related to the X-ray states of XTE J1650−500.

2.2. *X-Ray Observations*

In order to have a long-term view of the X-ray behavior of XTE J1650−500, we used the publicly available X-ray data from the *RXTE* ASM (Levine et al. 1996). The 1.5–12 keV ASM light curve is plotted in Figure 1. In addition, we also used PCA and HEXTE data from our pointed observations, as well as observations available from the *RXTE* archive. The procedure for reduction of these data can be found in Tomsick et al. (2003b, 2004). We used these data to extract count rates in the 3–200 keV band as a function of time. We define a hard color as the ratio of the HEXTE count rate (20–200 keV) to the 3–20 keV PCA count rate. We then constructed a hardness-intensity diagram (HID), similarly to Homan et al. (2003) and Rossi et al. (2004). We conducted a more detailed analysis of the X-ray energy spectrum for the *RXTE* observations closest in time to the eight radio observations. Using the XSPEC (ver. 11) software for spectral analysis, we fitted the PCA+HEXTE spectra, primarily to determine the fluxes in several energy bands (see Table 1, Figs. 5 and 6). In all cases, the spectral continuum is well described by a disk-blackbody (Makishima et al. 1986) plus power-law or cutoff power-law model, which is typical of BHC systems. We also accounted for interstellar absorption, and we fixed the column density to the value of $N_{\rm H} = 6 \times 10^{21}$ cm^{-2} measured by the *Chandra X-Ray Observatory* (Tomsick et al. 2004). For some observations, this continuum model left significant residuals near the iron Kα complex (6–10 keV), but we obtained acceptable fits with reduced $\chi^2 < 1.0$ after including an iron emission line and a smeared iron edge (Ebisawa et al. 1994). The final model we used to determine the

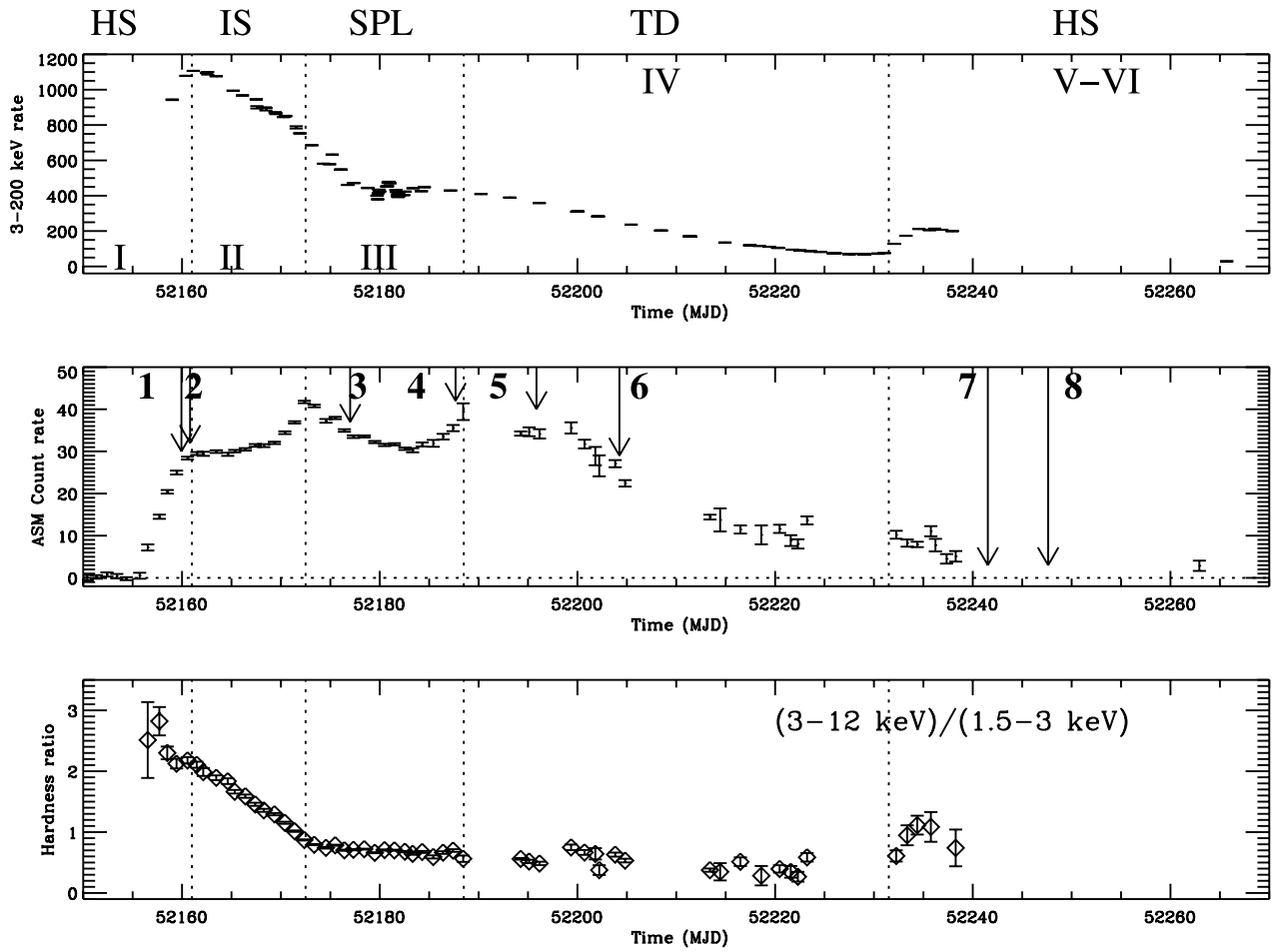

FIG. 1.—*Top*: *RXTE* (PCA+HEXTE) 3–200 keV count rate light curve (daily average) of XTE J1650−500 during its 2001–2002 outburst. *Middle*: *RXTE* ASM 1.5–12 keV count rate light curve. *Bottom*: Evolution of the ASM hardness ratio (3–12 keV/1.5–3 keV) during the whole outburst. The vertical dotted lines indicate the transition between the various X-ray states: HS (hard state), IS (intermediate state), SPL (steep power-law state), and TD (thermal dominant state). The roman numerals in the top panel illustrate the various time intervals used by Homan et al. (2003) and Rossi et al. (2004) for their X-ray analysis. The arrows (with a number) indicate when our radio observations were performed. We note that the high-frequency QPOs have been detected only in interval III (Homan et al. 2003).

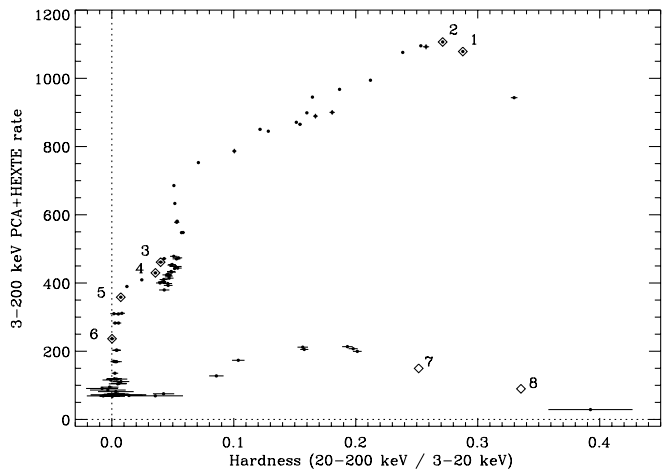

FIG. 2.—HID for the outburst of XTE J1650−500, similar to the one used by Homan et al. (2003). The diamonds (with associated number) indicate the period of simultaneous radio and X-ray observations. For observations 7 and 8, the position is only indicative, as XTE J1650−500 could not be observed by *RXTE* because of its proximity to the Sun. However (see text and Fig. 5), their positions are likely to be approximately correct.

X-ray fluxes is also described in detail in, e.g., Tomsick et al. (2001).

2.3. *The 2001–2002 X-Ray Outburst of XTE J1650−500*

To fully understand the radio properties of XTE J1650−500 during its outburst, we first need to characterize the X-ray states of XTE J1650−500 as a function of time. For that purpose, Figure 1 shows the *RXTE* ASM 1.5–12 keV and *RXTE* PCA+HEXTE 3–200 keV light curves, as well as the evolution of the *RXTE* ASM (3–12 keV/1.5–3 keV) hardness ratio; the arrows indicate the dates of the ATCA radio observations. In addition, the HID in Figure 2 adds complementary information on the outburst evolution; the diamonds highlight the radio observations. XTE J1650−500 moved counterclockwise in the HID during the whole outburst. As can be seen from these two figures, the scheduling of the radio observations provides a sampling of very different X-ray states of XTE J1650−500. In Figure 1 we indicate the time intervals used by Homan et al. (2003) and Rossi et al. (2004) with Roman numerals.

After its discovery on 2001 September 5 (MJD 52,157) by *RXTE* ASM (Remillard 2001), the first *RXTE* pointed observation occurred on 2001 September 6. The *RXTE* observations (up to September 9) are consistent with a BHC in the HS with a strong band-limited noise component in the power density

spectra and energy spectra dominated by a power-law component of photon index ∼1.6 and exponential cutoff (Revnivtsev & Sunyaev 2001; Wijnands et al. 2001). The rest of the bright outburst phase has been described by Rossi et al. (2004; S. Rossi 2004, private communication) and Homan et al. (2003), and we outline their conclusions below (for the decay phase, see Kalemci et al. [2003] and Tomsick et al. [2003b, 2004]). Starting around September 9, a gradual softening of the spectrum occurs up until October 5 (MJD 52,187). From September 9 to 20 (MJD 52,161–52,172), XTE J1650−500 is characterized by a smooth softening of its energy spectrum (with an evolution of the power-law photon index from 1.5 to 2.2), and the frequency of the QPO increases from ∼1 to 9 Hz. During the period from September 20 to October 5 (MJD 52,172–52,187), the photon index of the power-law component saturates to a value of ∼2.2. The rms variability and the frequency of the QPO become more erratic, with oscillations around their maxima. The high-frequency QPOs are observed only during this portion of the outburst (Homan et al. 2003). The accretion disk and power-law flux components give similar contributions to the total flux, which makes this interval very typical of the SPL state. We note that the photon index does not exactly fulfill the criteria (not greater than 2.4) of McClintock & Remillard (2004) for an SPL state, but as it is the part of the outburst with the steepest power law, we consider it as an SPL state for the rest of the paper. The properties of XTE J1650−500, between September 9 and 20, would then be consistent with an IS as defined above. From October 5 to November 19 (MJD 52,187–52,232), the contribution from the accretion disk dominates the energy spectra, and the level of rms variability is very low, as is typical of the TD state. XTE J1650−500 returned back to the HS after November 19 (MJD 52,232), as illustrated by the hardening of the spectrum and the increased rms variability (Kalemci et al. 2003; Rossi et al. 2004).

To summarize, after a brief (but we cannot exclude that the outburst was ongoing for many days before the discovery of the source) initial HS, XTE J1650−500 underwent a smooth transition to the IS, followed by transitions to the SPL state, the TD state, and then back to the HS. Our radio observations occurred as follows: observations 1 and 2 during the initial HS (however, observation 2 is very close to the transition to the IS), observations 3 and 4 during the SPL state (however, observation 4 is very close to the transition to the TD state), observations 5 and 6 during the TD state, and observations 7 and 8 during the final HS. A ninth observation was performed later, when XTE J1650−500 was back in quiescence. We now describe the properties of XTE J1650−500 within these X-ray states.

3. RADIO EMISSION FROM XTE J1650−500: RESULTS AND DISCUSSION

We now focus on the properties of the radio emission. We obtained radio coverage during the initial and final HSs, the SPL state, and the TD state. By looking at Table 1 and Figure 3, in which the radio light curve of XTE J1650−500 is plotted, we note that radio emission from XTE J1650−500 is detected during the first radio observation on September 7 with a spectrum consistent with being flat between 1384 and 2496 MHz. The day after, the radio flux density increased by almost a factor of 2 and had similar spectral characteristics. On September 24 we observed the source at a much fainter radio flux (∼0.8 mJy), and the source disappeared below the sensitivity level on October 5 with 3 σ upper limits of 0.21 and 0.18 mJy at 4800 and 8640 MHz, respectively. Compared to the brightest

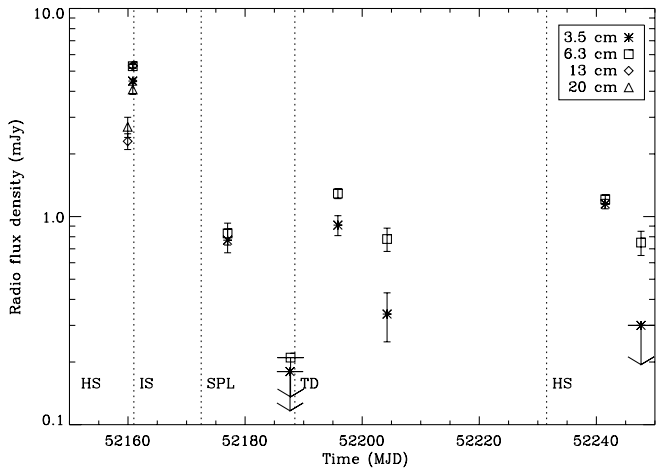

FIG. 3.—Radio light curve of XTE J1650−500 during its outburst in 2001. The vertical lines define the state transitions (see also Fig. 1). Upper limits are plotted at the 3 σ confidence level.

level of radio emission observed on September 8, this indicates a significant quenching (of more than a factor of 25) of the radio emission. Surprisingly, radio emission is again observed (observations 5 and 6) at the millijansky level in the TD state (contrary to expectations based on observations of other BHCs; e.g., Fender et al. 1999; Corbel et al. 2000). During the final two radio observations, the behavior of the source may be consistent with the behavior during the first two observations. For the rest of the paper, we define the radio spectral index α with $S_\nu \propto \nu^\alpha$, where S_ν is the radio flux density and ν is the frequency.

The best position of the radio counterpart to XTE J1650−500 (with the radio source fitted as a pointlike source) is $\alpha(\mathrm{J2000.0}) = 16^{\mathrm{h}}50^{\mathrm{m}}00^{\mathrm{s}}.96$, $\delta(\mathrm{J2000.0}) = -49^\circ 57' 44''.60$, with an absolute positional uncertainty of $0''.25$, mostly due to the uncertainty on the phase calibrator position. All radio observations (when the radio source is detected) are consistent with a location of the radio counterpart at this position. This constitutes the most accurate position for XTE J1650−500 and is in agreement with the one derived from optical observations (Castro-Tirado et al. 2001) and *Chandra* observations (Tomsick et al. 2004).

3.1. *The Initial and Final Hard States*

3.1.1. *Radio Emission from a Compact Jet*

Radio observations 1, 2, 7, and 8 were performed while XTE J1650−500 was in the HS. Both the initial and final hard X-ray states are therefore covered. Once again, the overall properties of the HS radio emission are broadly consistent with those that have been observed in other BHCs in a similar X-ray state (Corbel et al. 2000; Fender 2001): a level of radio emission of a few millijanskys with a radio spectrum that is almost flat. Such characteristics are believed to originate from a self-absorbed conical outflow or compact jet (e.g., Blandford & Königl 1979; Hjellming & Johnston 1988), similar to the one directly resolved from Cyg X-1 by Stirling et al. (2001). We do not detect linear polarization from the compact jet of XTE J1650−500, with our best 3 σ upper limit of 4.0% or 4.7% at 4800 or 8640 MHz, respectively. Such limits are consistent with previous detections at lower levels (e.g., Corbel et al. 2000 for GX 339−4).

For the purpose of our discussion, we have calculated the radio spectral indices, and these are included in Table 1.

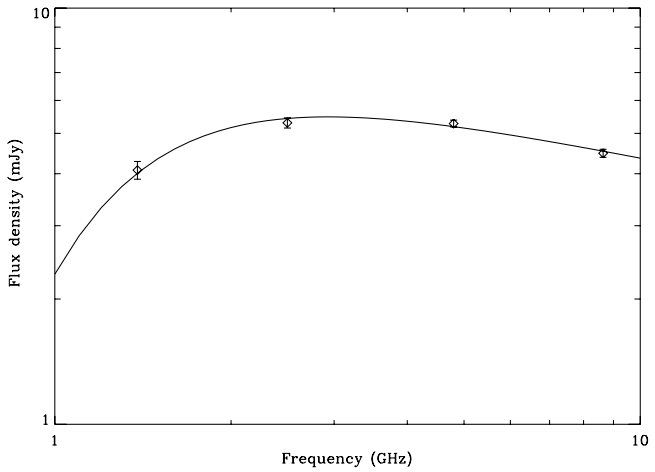

FIG. 4.—Radio spectrum of XTE J1650−500 for observation 2 on 2001 September 8. The solid line is the fit to a spectrum with a power law and thermal free-free absorption.

Despite being consistent with being flat ($\alpha \sim 0$), the radio spectrum (e.g., Fig. 4) seems less inverted at high radio frequencies than is typical for BHC systems.

Below, we come back to the last observation on December 4, which shows a very unusual spectrum. It is interesting to note that the radio spectrum on September 8 (observation 2: Fig. 4) shows a turnover at lower frequencies. This could be due to free-free absorption by a thermal plasma, and, indeed, a fit to the spectrum with a power law and free-free absorption [$S_\nu = S_0 \nu^\alpha \exp(-\tau \nu^{-2.1})$, where S_0 is the amplitude at 1 GHz, α is the spectral index of the unabsorbed spectrum, and τ is the free-free optical depth at 1 GHz] describes the data sufficiently well, with $S_0 = 8.59 \pm 0.07$ mJy, $\alpha = -0.29 \pm 0.04$, and $\tau = 1.32 \pm 0.02$. The opacity is in the range of values obtained by Fender (2001) for the 1989 outburst of V404 Cyg (GS 2023+338). We note that similarly, during the first detection of XTE J1859+226 in 1999, the radio spectrum also shows absorption at low frequencies (Brocksopp et al. 2002) while in the HS. If the radio emission arises from a compact jet (as is usually observed in the HS), then it is unlikely that synchrotron self-absorption is responsible for the observed absorption at low frequencies, as this emission originates from large-scale regions (see Fender 2001). The nature of the putative thermal absorbing plasma is unclear (higher interstellar medium [ISM] density, remnant of past activity, etc.). Alternatively (but probably less plausibly), the radio spectrum could be caused by two components: a flat component from the compact jet, as well as a second component from an optically thick ejection event. This may be a possibility, as radio observation 2 occurred very close to the hard to intermediate state transition. However, this is not favored by the fact that the radio spectra are all consistent with having the same intrinsic spectral index, even during the final HS (with the exception of observation 8). In addition, as discussed below, if an ejection event occurred for XTE J1650−500, it probably took place during the intermediate to SPL state transition (§ 3.2).

We note that the radio spectrum in observation 8 is very steep ($\alpha \leq -1.3$), and this is unusual for a black hole in the HS. It is not clear if this is related to the jet/ISM interaction mentioned below (likely not, as the spectrum in observation 7 looks similar to the initial HS) or possibly to the X-ray oscillation behavior observed 10 days later (Tomsick et al. 2003b).

As discussed above, we obtained the best constraint on the spectral index during the September 8 observation, with $\alpha = -0.29 \pm 0.04$. The reason the radio spectrum may have been less inverted than usual is still unclear. This may be related to the inclination angle of the jet, as usually lower inclination angles lead to flatter spectra (e.g., Falcke 1996). For example, the radio to millimeter spectrum of the compact jet of Cyg X-1 (a low-inclination system) is almost flat, i.e., $\alpha \sim 0$ (Fender et al. 2000). However, even with a low inclination angle for the jet, it is almost impossible to obtain such a negative spectral index. Furthermore, optical observations indicate that the inclination angle of the orbital plane in XTE J1650−500 is at least 50° (Orosz et al. 2004), so this explanation does not work for XTE J1650−500 unless the compact jets are strongly misaligned with the orbital plane (as might be the case in few systems; Maccarone 2002). In addition, we note that even in a system such as 4U 1543−47 with a low inclination angle ($20.^\circ7 \pm 1.^\circ0$; J. A. Orosz et al. 2005, in preparation), the radio spectrum of the compact jet (e.g., $\alpha = 0.08 \pm 0.04$) is still slightly inverted (Kalemci et al. 2004b). We also note that the spectral index also varies within a single source (e.g., GX 339−4; Corbel et al. 2000), so it is unlikely that the inclination angle is responsible for this less inverted radio spectrum.

According to Hjellming & Johnston (1988), a less inverted radio spectrum would also be expected in the case of lateral expansion slowed by an external medium (i.e., a compact jet with a narrower opening angle). In addition, because of the longitudinal pressure gradient, the bulk Lorentz factor would increase along the jet axis. If observers were looking into the jet boosting cone, they would expect to see an increase in low-frequency radio emission (which originates far from the base of the jet) and therefore possibly a much less inverted radio spectrum (e.g., Falcke 1996). Obscuration of part of the receding jet may also contribute to the nature of the spectrum. In any case, a combination of all these effects may be in place in XTE J1650−500. It is also clear that future studies of the evolution of the radio spectral index of the compact jets in BHC systems are important, as they may shed light on the geometry of the system.

If the measured spectral index is correct, then it is likely that the contribution from the compact jet at higher frequencies will not be significant. As illustrated in GX 339−4 and XTE J1550−564, the spectrum of the compact jet extends to shorter wavelengths, with a transition to the optically thin regime in the near-infrared (Corbel et al. 2001; Corbel & Fender 2002). In that case, it is unlikely that an infrared reflare would have been detected during the soft to hard state transition, as in XTE J1550−564, GX 339−4, or 4U 1543−47 (Jain et al. 2001; Buxton & Bailyn 2004). The contribution in X-ray, as direct synchrotron emission (e.g., Markoff et al. 2001, 2003), may also be negligible (see § 3.1.2); however, a contribution from synchrotron self-Compton (SSC) emission from the base of the compact jet (e.g., Markoff & Nowak 2004) cannot be ruled out at this stage.

3.1.2. *On the Radio/X-Ray Correlation*

While in the HS, BHCs display a strong correlation between their radio and X-ray emission. This was first observed in GX 339−4 (Corbel et al. 2000, 2003) over more than 3 orders of magnitude in X-ray flux and almost down to its quiescence level. Gallo et al. (2003) found a similar correlation for GS 2023+338 (V404 Cyg), but, interestingly, they show that all BHCs in the HS behave similarly, i.e., their data are consistent with a universal relation between radio and X-ray luminosities. They also observed a relatively small scatter of approximately

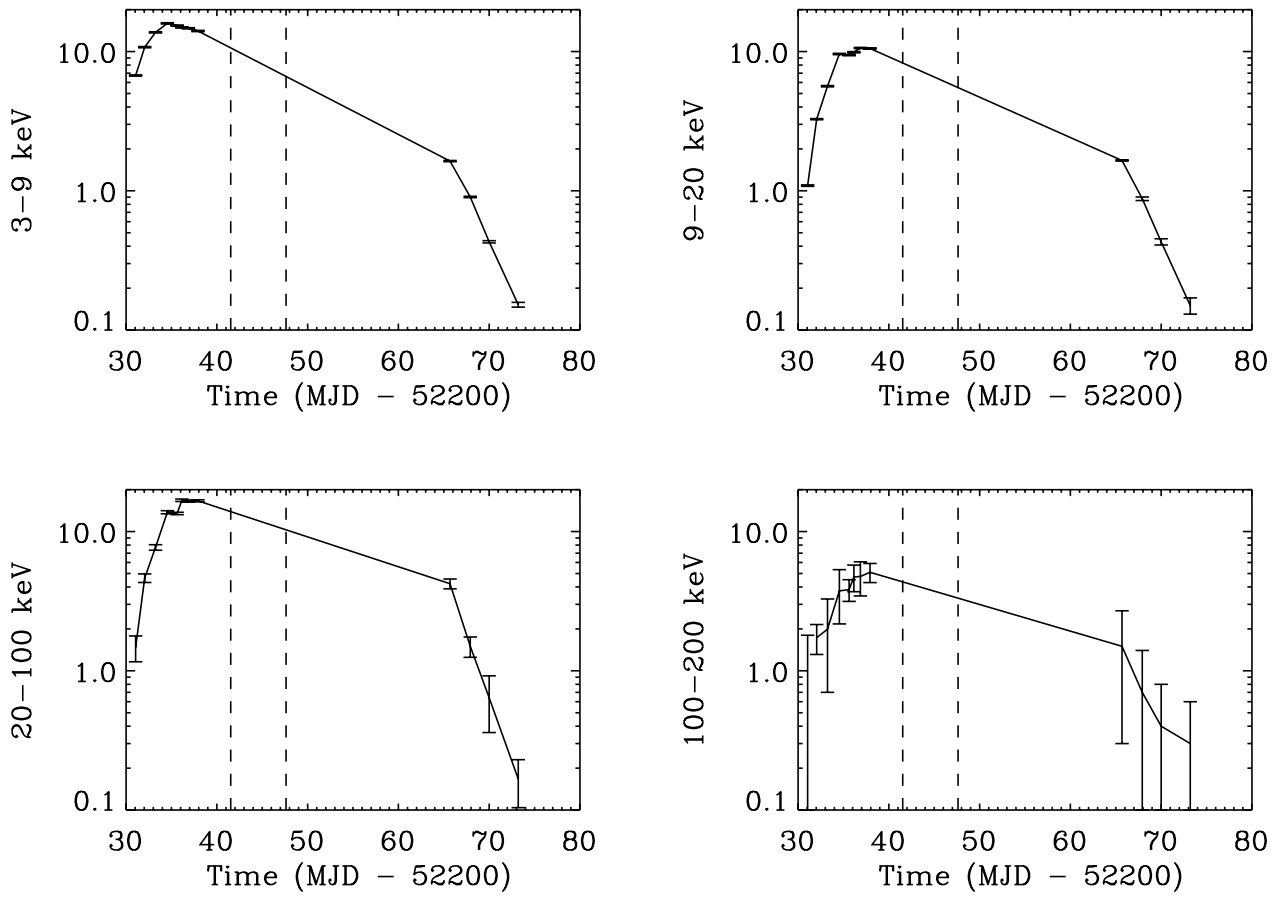

FIG. 5.—Evolution of the X-ray flux (in units of 10^{-9} ergs s^{-1} cm^{-2}) in various energy bands during the decay phase. The transition from the TD state to the HS occurred on MJD 52,232. The dashed vertical lines indicate when radio observations 7 and 8 were performed. These figures give a feeling for the precision of our X-ray flux estimates (for radio observations 7 and 8) based on an interpolation of the decay trend.

1 order of magnitude in radio power. In fact, the scatter could be even smaller if we account for the recent distance estimate, in the range between 6 and 15 kpc, for GX 339−4 by Hynes et al. (2004), as this will bring GX 339−4 closer to GS 2023+338, and the small scatter could imply low bulk Lorentz factors (<2) for the compact jets. Interestingly, this correlation also seems to hold for a large sample of supermassive black holes if one takes into account the mass of the black hole as an additional correction (Merloni et al. 2003; Falcke et al. 2004).

In order to see if XTE J1650−500 fits into this picture, we looked at the relationship between the X-ray and radio flux levels for XTE J1650−500. Despite our efforts to get quasi-simultaneous X-ray and ATCA observations (see Table 1), this was not possible for the final HS, as XTE J1650−500 was in the solar exclusion zone for *RXTE*. In Figure 5 we plot the X-ray flux in various bands during a portion of the decay of the 2001 outburst (see also Tomsick et al. 2003b, 2004). After the transition to the HS (on MJD 52,232; Kalemci et al. 2004a), the decay is smooth enough that interpolation of the X-ray flux at the time of the radio observation is sufficient to obtain an estimate. We note that an increase of the decay rate is observed at the end of the outburst (Fig. 5), with a spectrum that gets harder with time (a smooth variation of the photon index: 1.91 ± 0.02 on MJD 52,235.6 to 1.35 ± 0.23 on MJD 52,267.9), very similar to the decay of XTE J1908+094 during its 2003 outburst (Jonker et al. 2004).

In Figure 6 we have plotted the radio flux density at 4.8 GHz versus the unabsorbed 2–11 keV X-ray flux (in Crab units) scaled to a distance of 1 kpc (similar to Gallo et al. 2003),

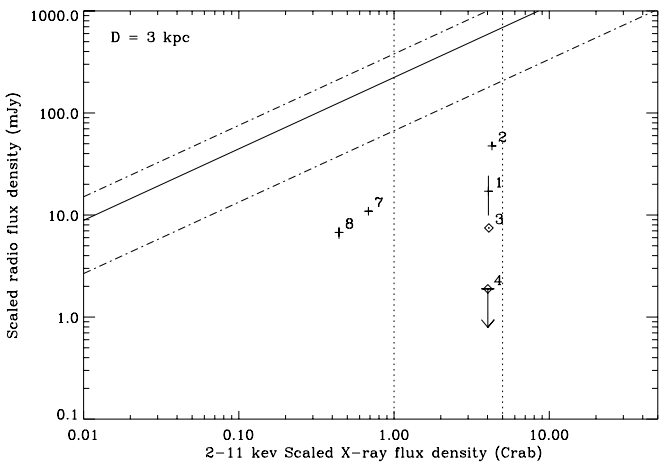

FIG. 6.—Radio flux density (mJy) at 4.8 GHz of XTE J1650−500 during the HS and SPL state vs. the unabsorbed 2–11 keV X-ray flux (in Crab units) scaled to a distance of 1 kpc (this assumes that XTE J1650−500 is located at 3 kpc from the Earth). As described in the text, the X-ray fluxes for observations 7 and 8 are from an interpolation of the decay trend. The best-fit function (*solid line*) with its associated error (*dot-dashed lines*), obtained by Gallo et al. (2003) for GX 339−4 and GS 2023+338, are also plotted. The vertical dotted lines indicate the level of 2% and 10% Eddington luminosity for a 4 $M_{\odot}$ black hole.

assuming a distance of 3 kpc for XTE J1650−500. This distance gives luminosity estimates during the state transition consistent with other BHCs (Maccarone 2003). In Figure 6 we have also plotted the best-fit function obtained by Gallo et al. (2003) using their data sets, i.e., $S_{\rm radio} = k(S_x)^{+0.7}$, with $k = 223 \pm 156$ mJy. Although we have a sample of only four data points, we can clearly see that they all lie significantly below (by a factor 20) the best-fit line of Gallo et al. (2003). The determination of the slope of the power-law function linking the radio and X-ray emission is very uncertain because of our limited sample of data points (as well as the unusual radio spectrum in observation 8 and the fact that two observations took place very close to state transitions). The reason that the normalization in XTE J1650−500 is significantly lower (the source is less radio loud or more X-ray loud) than in other BHCs (Gallo et al. 2003) is still unclear. It may be related to the fact that direct synchrotron X-ray emission (and possibly even SSC) from the compact jets is likely not dominant in the case of XTE J1650−500 for a reason that still remains to be explained. The lower normalization in XTE J1650−500 could be related to the fact that the X-ray regime may be dominated by thermal Comptonization of disk photons in the corona. We note that the distance to XTE J1650−500 may be larger than 3 kpc, but this will only make XTE J1650−500 more anomalous relative to the other BHCs.

3.2. *Radio Emission in the Intermediate and Steep Power-Law States*

3.2.1. *The Steep Power-Law State of XTE J1650−500*

As outlined above, after a few days in the HS, XTE J1650−500 entered the IS and then went into the SPL state. In the IS, the X-ray spectrum softens gradually until the photon index reaches a value of ∼2.2 (Rossi et al. 2004), whereas the QPO frequency increases from 1 to 8.5 Hz. Then (SPL state), the photon index and the QPO frequency (it is not clear if this is the same type of QPO) oscillate around their saturation value. This behavior is more pronounced for the QPO frequency, as it fluctuates along with the broadband variability. The slow variations of the photon index could be related to cooling of the corona by an increase in the number of soft disk photons (the inner accretion disk could get closer to the black hole). Significant variations are also observed in the total disk flux contribution (Rossi et al. 2004) and may indicate that the accretion disk has reached the innermost stable circular orbit (ISCO) and is oscillating around this value. This interval (SPL state) also corresponds to the period over which high-frequency QPOs are detected and therefore confirms that the disk is very close to the black hole (Homan et al. 2003).

We conducted two radio observations during the SPL state of XTE J1650−500 in 2001. The first one resulted in the detection of XTE J1650−500 at a faint level of ∼0.8 mJy (the spectral index is not well constrained: $\alpha = -0.13 \pm 0.86$). The second observation did not result in a detection of XTE J1650−500, with 3 σ upper limits of 0.18 mJy at 8640 MHz and 0.21 mJy at 4800 MHz, indicating a significant (more than a factor of 25) quenching of radio emission compared to the initial HS.

3.2.2. *The Steep Power-Law State of XTE J1550−564 and XTE J1859+226*

Very few soft X-ray transients have been observed at radio frequencies during the intermediate or SPL states. Moreover, when these states have been observed, the radio emission has usually been dominated by the decaying optically thin synchrotron emission arising from jet ejections that occur at or near state transitions prior to the source entering the intermediate or SPL state. Thus, when the emission from the jet ejections is detected, it is decoupled from the black hole system, implying that the observed radio emission is not an intrinsic property of the intermediate or SPL states, as the emitting electrons are already far from the system.

There is only one case for which the radio observations sampled the intrinsic properties of the intermediate or SPL states: XTE J1550−564 during its reactivation in 2000 (Corbel et al. 2001). Interestingly, the properties of the radio emission from XTE J1550−564 were quite similar to what we observe now in XTE J1650−500; indeed, for XTE J1550−564 the first detection showed an optically thin spectrum with a well-constrained spectral index of $\alpha = -0.45 \pm 0.05$, while later, the radio emission was quenched. The optically thin component was interpreted as synchrotron emission arising from relativistic plasma during the state transition. Such small ejection events are frequently observed during state transitions (e.g., see Fender et al. [1999] or Corbel et al. [2000] for the 1998 outburst of GX 339−4 or Brocksopp et al. [2005] for the 2003 outburst of XTE J1720−318). We note that the spectacular massive ejection events (with bright radio emission and a radio core that is usually resolved on a timescale of weeks; e.g., Mirabel & Rodríguez [1994] for GRS 1915+105) may be related to sharper state transitions, possibly related to a huge increase in the accretion rate in the inner part of the accretion disk or maybe to a different black hole parameter, such as the spin.

Furthermore, we highlight the fact that during the 1999 outburst of XTE J1859+226, Brocksopp et al. (2002) reported the detection of flaring radio emission from this black hole in a soft state, which is unexpected in the canonical high/soft (or TD) state (e.g., Fender et al. 1999). In that case, the radio flaring emission was clearly associated with spectral hardening of the X-ray spectrum. However, their definition of a soft state is not clear. Indeed, the hard X-ray light curve in Brocksopp et al. (2002) revealed a very significant level of hard X-ray emission up to at least MJD 51,490, which is very uncommon for a TD state (e.g., McClintock & Remillard 2004). In addition, Cui et al. (2000) reported the detection of high-frequency QPOs around MJD 51,468, which is a characteristic of the SPL state (McClintock & Remillard 2004); this is also favored by the large fraction of X-ray flux in the power-law component (Hynes et al. 2002), which is also quite steep. Kalemci (2002), analyzing the *RXTE* PCA data of XTE J1859+226 after MJD 51,515, describes the spectral state evolution as a TD state from MJD 51,515 up to 51,524, after which the system was found in the IS for the remaining PCA observations. Based on the above, it seems likely that the TD state in XTE J1859+226 did not start before MJD 51,490. This is confirmed by Markwardt (2001), as this work indicates that the disk component became dominant only after MJD 51,487. Therefore, the X-ray state in which Brocksopp et al. (2002) detected flaring radio emission from XTE J1859+226 was most likely the SPL state (or less probably an IS) and not a TD state. Therefore, the observed radio flaring behavior in XTE J1859+226 must be related to the behavior of BHCs while in the SPL state. This conclusion has also been drawn by Fender et al. (2005).

3.2.3. *XTE J1650−500 and the Origin of Radio Emission in the Steep Power-Law State*

With our new observations, XTE J1650−500 is therefore the third source for which the intrinsic radio properties of the SPL state have been sampled, and the observed behavior is consistent with what has been found in XTE J1550−564 (Corbel

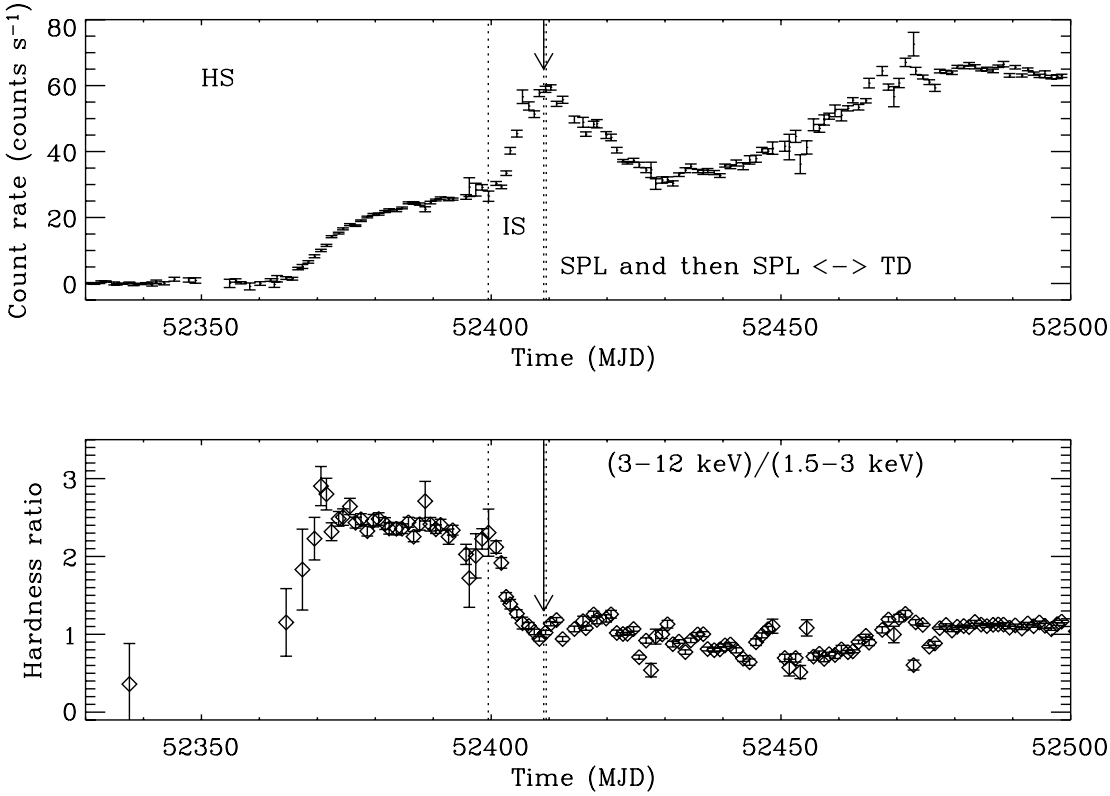

FIG. 7.—Evolution of the *RXTE* ASM count rate and hardness ratio (similar to Fig. 1) for the initial part of the 2002 outburst of GX 339−4. Again, the X-ray spectral states sampled (T. Belloni 2004, private communication) are indicated. The arrow marks the time of the major radio flare observed by Gallo et al. (2004) in 2002 May.

et al. 2001). The detection of the faint radio component in the SPL state on September 24 (observation 3) may be related to an ejection event at the time of the transition from the hard to intermediate states (on September 9). However, as there is significant time (15 days) between the transition and the detection of the faint radio component, we consider two alternative explanations.

First, an interesting comparison can be made with the 2002–2003 outburst of GX 339−4, as a strong radio flare has been observed with ATCA (Gallo et al. 2004). In Figure 7 we have plotted the ASM light curve and hardness ratio (similar to Fig. 1 for XTE J1650−500) for the initial part of the outburst. As GX 339−4 and XTE J1650−500 have similar hydrogen column densities (e.g., Miller et al. 2004), we can directly compare their hardness ratios, which are indeed very similar (Figs. 1 and 7). After an initial HS, GX 339−4 makes a transition to an IS around MJD 52,400. Then, the spectrum softens up to approximately MJD 52,409, when GX 339−4 is found in the SPL state. The evolution of the states becomes more complicated later on in the outburst (T. Belloni 2004, private communication). The spectral state evolution (during the beginning of the outburst) in GX 339−4 is therefore identical to that of XTE J1650−500. The radio flare observed by Gallo et al. (2004) started on 2002 May 14 around 13:00 (MJD 52,409.042), reaching its maximum 6 hr later. The arrow in Figure 7 indicates that the radio flare started once the softening of the X-ray spectrum ended, i.e., it corresponds to the transition from the IS to the SPL state. Based on the above, and comparing their hardness ratios, we can say that if a radio flare (and hence massive plasma ejection) occurred in XTE J1650−500, then this happened at the transition between the IS and SPL state. In that case, the observed radio emission on September 24 would have been at the end of the decay of this flare. This could correspond to the ejected materials that later interacts with the ISM (§ 3.3), as in GX 339−4 (Gallo et al. 2004).

Alternatively, an equally plausible explanation is the following. The transition from the IS to the SPL state seems to correspond to a period over which the inner radius of the accretion disk reaches the ISCO, and this would be valid for most of the SPL state, as outlined above in § 3.2.1. As the X-ray properties of the SPL state favor an "unstable" accretion disk (Rossi et al. 2004), they may suggest that the optically thin synchrotron component observed on September 24 could be related to an ejection of a very small portion of the inner accretion disk or corona. In that case, it would be very similar to the radio flaring behavior observed in XTE J1859+226 during its SPL state in 1999 or to the behavior observed in GRS 1915+105 (but at a much slower rate). The comparison of GRS 1915+105 with BHCs in canonical X-ray states is not straightforward, but the X-ray states A, B (soft), and C (hard) may be similar to intermediate and very high states (Reig et al. 2003). Oscillations between states A, B, and C are correlated with radio flaring activity (e.g., Klein-Wolt et al. 2002), with stronger radio emission in the spectrally hard state C, whereas the soft states are never associated with bright radio emission.

These two possible explanations for the origin of radio emission in the IS and SPL state could be combined as follows: For GX 339−4 and probably for XTE J1650−500, the transition from the IS to the SPL state is associated with an ejection event (with a radio spectrum characteristic of optically thin synchrotron emission) that decays on a timescale of hours. After the transition, the accretion disk settles down close to the ISCO. At that time, as the spectrum hardens, accretion disk or coronal material can be ejected from the system (as in XTE J1859+226), resulting in weak radio flares. If the radio observation takes place between two flares, then no radio emission will be observed. Indeed, this

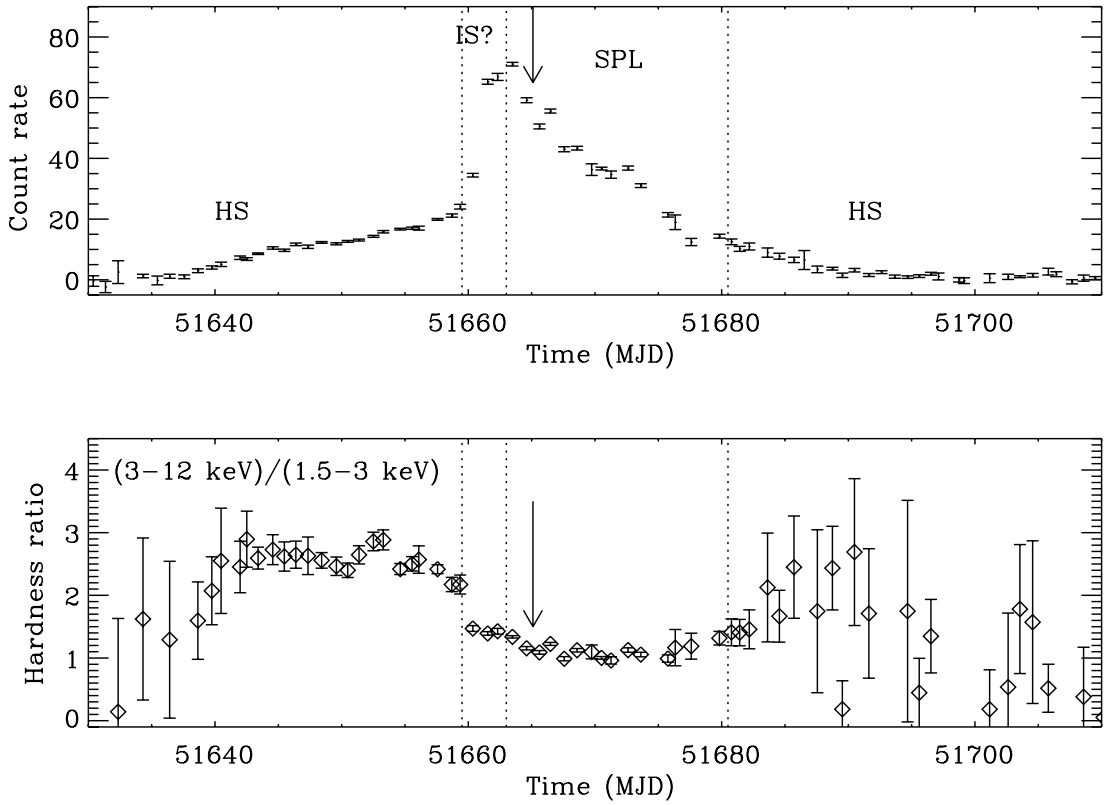

FIG. 8.—Same as Fig. 7, but for the 2000 outburst of XTE J1550−564. The arrow indicates the date of the radio observations performed by Corbel et al. (2001), during which they probably detected the end of the radio flare associated with the state transition. The high-frequency QPOs are detected only during the SPL state.

was also the case for GX 339−4: after the major radio flare associated with the IS to SPL state transition, several radio flares were observed during the SPL state (Gallo et al. 2004), and, interestingly, for at least one SPL state radio observation (on 2002 June 9 [MJD 52,434]), the radio emission was quenched (by a factor of more than 45 compared to the initial HS).

Indeed, we can now try to see if the 2000 radio observations of XTE J1550−564 fit into this framework. For that purpose, we have plotted in Figure 8 the ASM hardness ratio and light curve for the 2000 outburst. Similarly, after an initial HS (e.g., Rodriguez et al. 2003, 2004), the source went into the SPL state with gradual softening of the X-ray spectrum in between (very similar to the IS of XTE J1650−500 and GX 339−4 mentioned above). The radio flare was observed again after the softening was over (Corbel et al. 2001). Again, the high-frequency QPOs (Miller et al. 2001) were reported in only the SPL state (between MJD 51,663 and 51,672), i.e., after the end of the softening. The second radio observation of XTE J1550−564 occurred later in the SPL state and showed that the radio emission was quenched, so that either the observation occurred between two flares or perhaps there was no flare at all. The X-ray spectral evolution (Rodriguez et al. 2003) may even suggest that the ejected material could be originating from the corona. The outburst evolution of XTE J1859+226 (Fig. 9) could again be included in this picture in this way: after an initial HS and a softening, a massive radio flare occurred, and then, as the source became spectrally harder, several weaker flares took place.

3.2.4. *On the Nature of Radio Emission in the Intermediate State*

At this stage, it is not clear if the general pattern presented in § 3.2.3 concerns only the SPL state. Perhaps the IS, with slower evolution and a significant level of hard X-ray emission (like the IS in XTE J1650−500), is not associated with radio emission. In fact, it is interesting to note that before the major radio flare observed in 2002 (see Fig. 2 in Gallo et al. 2004), a stable level of radio emission with a flux of ∼12 mJy and a flat spectrum (between 4.8 and 8.6 GHz) was observed in GX 339−4. Therefore, as GX 339−4 was in the IS at that time, this would indicate that the compact jet could possibly survive during the IS but could be destroyed very quickly, i.e., on a timescale of hours. Similarly, a nonzero level of radio emission with a flat spectrum is also observed in XTE J1859+226 prior to its major radio flare in 1999 (Brocksopp et al. 2002). Again, this detection would be consistent with the presence of the compact jet in the IS of XTE J1859+226. If this interpretation is correct (i.e., that the compact jet exists in the IS), this would be an important clue for understanding the inflow-outflow coupling close to the event horizon of a black hole. For that purpose, it would be very important to monitor the radio properties of BHCs during the IS or SPL state in order to constrain the geometry of these BHC systems during the various X-ray states. In any case, this suggestion seems to be confirmed by Fender et al. (2005), who studied similar data sets (including also GRS 1915+105 but not XTE J1650−500) and drew similar conclusions regarding the nature of radio emission in the IS and SPL state.

3.2.5. *Quenched Radio Emission at a Few Percent Eddington Luminosity*

As a final remark, in Figure 6 we observe that the radio observations in the initial HS and in the SPL state occurred at the same unabsorbed X-ray flux, which corresponds to a level of 4 Crab (∼8% of the Eddington luminosity for a 4 $M_{\odot}$ black hole at 3 kpc; if we used an upper limit of 7 $M_{\odot}$, then it would correspond to about 4.6% of the Eddington luminosity). This

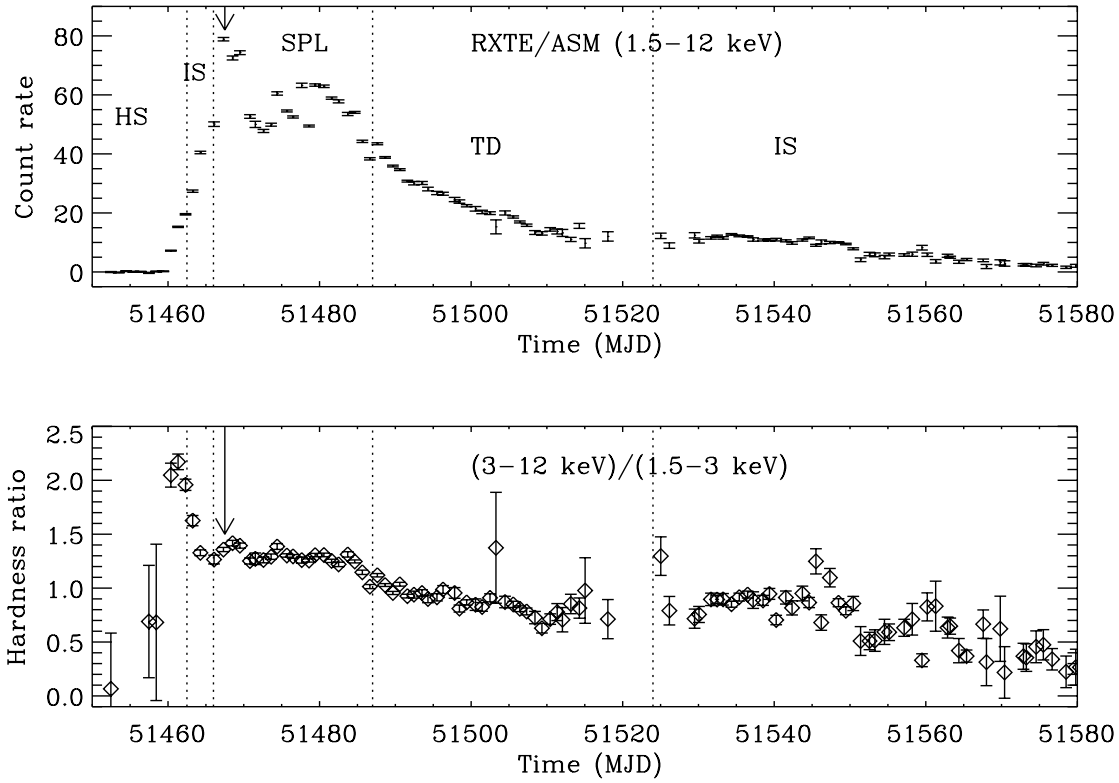

FIG. 9.—Same as Fig. 7, but for the 1999 outburst of XTE J1859+226. The arrow indicates the date of the major radio flare detected by Brocksopp et al. (2002). The first two vertical lines, for the HS and IS, are approximately indicative of the period of state transitions.

picture is qualitatively consistent with the behavior of GX 339−4, Cyg X-1, and GS 2023+338 (Gallo et al. 2003), indicating that the quenching of the compact jet occurs at an almost fixed fraction (a few percent) of the Eddington luminosity, so that there is a correlation between the mass of the black hole and the X-ray flux where the transition occurs. We note that if the mass of a black hole is known, then a measurement of the X-ray flux for which quenching occurs could constitute an independent distance estimate (or vice versa).

3.3. *Surprising Detection of Radio Emission in a Thermal Dominant State*

The last radio observations that we discuss in this paper are those (5 and 6) that were conducted during the TD state. Radio emission is observed (Figs. 3 and 10) at a level of $\sim$1 mJy, with a spectrum that is consistent with optically thin synchrotron emission (but the spectral index is not well constrained). These detections are contrary to what would have been expected in the TD state, which has always (in previous observations of BHCs) been associated with quenched radio emission: e.g., GX 339−4 (Fender et al. 1999; Corbel et al. 2000) and Cyg X-1 (Gallo et al. 2003; Tigelaar et al. 2004). Therefore, these detections do not fit with the standard view, and they constitute a certain surprise. As discussed in § 3.2, the radio flaring emission observed in the soft state of XTE J1859+226 (Brocksopp et al. 2002) has to be related to the behavior of the BHC while in the SPL state. Regarding the case of XTE J1650−500, the HID (Fig. 2) indicates that the detection of radio emission in the TD state is not related to spectral hardening at all, as the X-ray emission stays very soft during this period, with no hard component. Therefore, an alternative explanation must be found, and we concentrate on two possibilities.

First, we consider the possibility that the radio emission is still related to the compact jet. As demonstrated in the case of GX 339−4 (Fender et al. 1999; Corbel et al. 2000), the TD state is associated with a quenching of the compact jet by at least a factor of 25. According to Meier et al. (2001), the quenching would be the result of a weaker poloidal magnetic field in a geometrically thin accretion disk. Migliari et al. (2004) reported the detection of radio emission in two atoll-type neutron star

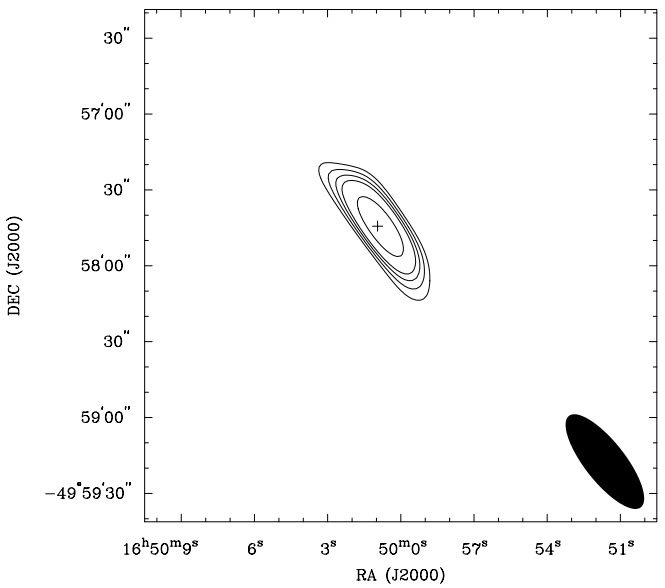

FIG. 10.—Radio emission at 8640 MHz during an observation performed on MJD 52,195 (observation 5) in a TD state. Contours are at 3, 4, 5, 7, and 9 times the rms level of 0.10 mJy beam^{-1}.

TABLE 2
PROPERTIES OF RADIO EMISSION ALONG THE VARIOUS X-RAY STATES IN XTE J1650−500 AND IN BLACK HOLE BINARY SYSTEMS IN GENERAL

X-RAY STATE	ORIGIN OF THE RADIO EMISSION	
	XTE J1650−500	Black Hole Candidates
HS	Self-absorbed compact jet	Self-absorbed compact jet
IS	No radio observation	Self-absorbed compact jet
IS to SPL state transition	No radio observation	Massive ejection event
SPL state	Decay of massive ejection event or small ejection event and quenching	Small ejection events and/or quenched radio emission
TD state	Interaction jet/ISM?	Quenched radio emission

NOTES.—See also Fender et al. (2005) for the general case. We note that in any state observed after the IS to SPL state transition, radio emission from the interaction of the massive ejection event with the ISM may contribute to the observed level of radio emission (if unresolved).

X-ray binaries while they were in a soft (banana) X-ray state. They suggested that this could be related to an interaction of the magnetic field of the neutron star with the accretion disk. However, such an explanation does not work in the case of XTE J1650−500, which is likely a black hole, based on its X-ray properties and also its mass function (Orosz et al. 2004). Perhaps the mass of the black hole in XTE J1650−500 (which may be smaller than a typical stellar-mass black hole) is an important parameter that could set the level of quenching when the spectrum gets soft. However, as the compact jet was quenched by a factor of more than 25 in the SPL state (observation 4), similar to other BHCs (e.g., GX 339−4; Fender et al. 1999), it seems likely that the observed radio emission in the TD state of XTE J1650−500 does not originate from the compact jet.

The second possibility that we consider now is that the observed radio emission is the result of the interaction of material previously ejected from the system with the ISM, similarly to what has been observed for XTE J1550−564 (Corbel et al. 2002; Tomsick et al. 2003a; Kaaret et al. 2003) and for GX 339−4 (Gallo et al. 2004). The observed radio spectrum would be consistent with this interpretation (optically thin synchrotron emission, but it should be kept in mind that the spectral index is not well constrained). In addition, we have also observed that within an observation, the flux is varying (decaying) on a timescale of hours. For example, in observation 5, the radio flux density drops (during the observation) from 1.74 ± 0.11 to 0.85 ± 0.11 mJy at 4800 MHz and from 1.09 ± 0.11 to 0.80 ± 0.15 mJy at 8640 MHz. There also seems to be some variations for observation 6.

This is contrary to what has been found previously in XTE J1550−564, with the slow decay of radio emission (on a timescale of a week) due to the jet/ISM interaction (Corbel et al. 2002; S. Corbel et al. 2005, in preparation). However, the variations of radio emission in the large-scale jet of GX 339−4 were much faster than in the case of XTE J1550−564. The origin of the ejected material could be related to the flaring behavior in the SPL state, or more likely during the IS to SPL state transition (as discussed in § 3.2), similarly to GX 339−4. If this interpretation were correct, the contribution to the X-ray spectrum of the interaction of the jet with the ISM (as in XTE J1550−564) would not be detectable, as the X-ray spectrum would likely be dominated by the thermal emission from the accretion disk. In any case, this may suggest that the reactivation of particle acceleration during collisions with the ISM may be a common occurrence in microquasars.

4. CONCLUSIONS

XTE J1650−500 was discovered in 2001 September and then underwent transitions between various X-ray spectral states while we observed the source at radio frequencies. We can summarize our conclusions as follows: In the HS, the radio emission of XTE J1650−500 can be interpreted (like other BHCs) as arising from a self-absorbed compact jet. However, there seems to be some indication that the radio spectrum is less inverted than in other sources. In addition, XTE J1650−500 seems to be more X-ray loud when compared to other black hole candidates observed at similar radio flux density. This could possibly indicate that XTE J1650−500 is dominated in the X-ray regime by Comptonization of the disk photons in the corona with negligible (if any) contribution from the compact jet at high energies (X-ray, optical, and possibly even in the infrared). With the observations performed in the SPL state and using the existing data from other BHCs, we conclude that the transition from the IS to the SPL state is likely associated with a (more or less) massive ejection event that decays on a timescale of hours. In addition, weaker radio flares (and hence ejection events) may be observed in the SPL state associated with X-ray spectral hardening. If a radio observation took place between two flares or if no flare occurred at all, then no radio emission would be detected. For the IS itself, the detection of radio emission (with a flat spectrum) prior to the major flare of XTE J1859+226 in 1999 and of GX 339−4 in 2002 (associated with an IS to SPL state transition) may suggest that the compact jet can survive in the IS, and perhaps this is due to the fact that the flux of soft X-rays is lower in the IS than in the SPL state. In the TD state, we have surprisingly detected a significant amount of varying radio emission, which we interpret as the interaction of previously ejected materials with the neighboring environment (ISM or a remnant of past activity), similar to what has been observed in XTE J1550−564. In that case, such events may be more common than previously thought. Our conclusions regarding the nature of radio emission within the various spectral states of XTE J1650−500 and a possible extension to BHCs in general are summarized in Table 2. All of this points to the fact that it is extremely important to intensively monitor the radio properties of BHCs along the various X-ray states in order to shed light on the accretion-ejection coupling close to the black hole event horizon.

The Australia Telescope is funded by the Commonwealth of Australia for operation as a national facility managed by CSIRO. *RXTE* ASM results are provided by the *RXTE* ASM team at the Massachusetts Institute of Technology. We thank Bob Sault, Dave McConnell, and the ATCA time allocating committee for allowing these observations at the right times to sample various X-ray states. S. C. acknowledges useful and

interesting discussions with Heino Falcke, Elena Gallo, Sera Markoff, Mike Nowak, and Jerry Orosz. S. C. would like to thank Dick Hunstead and Duncan Campbell-Wilson for providing information on the *MOST* observations, which helped to schedule the ATCA observations, and Bryan Gaensler and Jim Lovell for conducting some of the radio observations. We also warmly thank Sabrina Rossi and Tomaso Belloni for providing information on their PCA data analysis of XTE J1650−500 and GX 339−4, which helped in defining the state evolution. J. A. T. acknowledges partial support from NASA grant NAG5-13055.

REFERENCES

Augusteijn, T., Coe, M., & Groot, P. 2001, IAU Circ. 7710
Belloni, T. 2004, in The Restless High-Energy Universe, ed. E. P. J. van den Heuvel, J. J. M. in 't Zand, & R. A. M. J. Wijers (Amsterdam: North-Holland) (astro-ph/0309028)
Blandford, R. D., & Königl, A. 1979, ApJ, 232, 34
Brocksopp, C., Corbel, S., Fender, R. P., Rupen, M., Sault, R., Tingay, S. J., Hannikainen, D., & O'Brien, K. 2005, MNRAS, in press (astro-ph/0410353)
Brocksopp, C., et al. 2002, MNRAS, 331, 765
Buxton, M., & Bailyn, C. 2004, in AIP Conf. Proc. 714, X-Ray Timing 2003: Rossi and Beyond, ed. P. E. Kaaret & F. Lamb (New York: AIP), 146
Castro-Tirado, A. J., Kilmartin, P., Gilmore, A., Petterson, O., Bond, I., Yock, P., & Sanchez-Fernandez, C. 2001, IAU Circ. 7707
Corbel, S., & Fender, R. P. 2002, ApJ, 573, L35
Corbel, S., Fender, R. P., Tzioumis, A. K., Nowak, M., McIntyre, V., Durouchoux, P., & Sood, R. 2000, A&A, 359, 251
Corbel, S., Fender, R. P., Tzioumis, A. K., Tomsick, J. A., Orosz, J. A., Miller, J. M., Wijnands, R., & Kaaret, P. 2002, Science, 298, 196
Corbel, S., Nowak, M. A., Fender, R. P., Tzioumis, A. K., & Markoff, S. 2003, A&A, 400, 1007
Corbel, S., et al. 2001, ApJ, 554, 43
Cui, W., Shrader, C. R., Haswell, C. A., & Hynes, R. I. 2000, ApJ, 535, L123
Ebisawa, K., et al. 1994, PASJ, 46, 375
Falcke, H. 1996, ApJ, 464, L67
Falcke, H., Körding, E., & Markoff, S. 2004, A&A, 414, 895
Fender, R. P. 2001, MNRAS, 322, 31
Fender, R. P., Belloni, T., & Gallo, E. 2005, ApJ, in press (astro-ph/0409360)
Fender, R. P., Pooley, G. G., Durouchoux, P., Tilanus, R. P. J., & Brocksopp, C. 2000, MNRAS, 312, 853
Fender, R. P., et al. 1999, ApJ, 519, L165
Gallo, E., Corbel, S., Fender, R. P., Maccarone, T. J., & Tzioumis, A. K. 2004, MNRAS, 347, L52
Gallo, E., Fender, R. P., & Pooley, G. G. 2003, MNRAS, 344, 60
Groot, P., Tingay, S., Udalski, A., & Miller, J. 2001, IAU Circ. 7708
Hjellming R. M., & Johnston K. J. 1988, ApJ, 328, 600
Homan, J., Klein-Wolt, M., Rossi, S., Miller, J. M., Wijnands, R., Belloni, T., van der Klis, M., & Lewin, W. H. G. 2003, ApJ, 586, 1262
Homan, J., Wijnands, R., van der Klis, M., Belloni, T., van Paradijs, J., Klein-Wolt, M., Fender, R., & Méndez, M. 2001, ApJS, 132, 377
Hynes, R. I., Haswell, C. A., Chaty, S., Shrader, C. R., & Cui, W. 2002, MNRAS, 331, 169
Hynes, R. I., Steeghs, D., Casares, J., Charles, P. A., & O'Brien, K. 2004, ApJ, 609, 317
Jain, R. K., Bailyn, C. D., Orosz, J. A., McClintock, J. E., & Remillard, R. A. 2001, ApJ, 554, L181
Jonker, P. G., Gallo, E., Dhawan, V., Rupen, M., Fender, R. P., & Dubus, G. 2004, MNRAS, 351, 1359
Kaaret, P., Corbel, S., Tomsick, J. A., Fender, R., Miller, J. M., Orosz, J. A., Tzioumis, A. K., & Wijnands, R. 2003, ApJ, 582, 945
Kalemci, E. 2002, Ph.D. thesis, Univ. California, San Diego
Kalemci, E., Tomsick, J. A., Rothschild, R. E., Pottschmidt, K., Corbel, S., Wijnands, R., Miller, J. M., & Kaaret, P. 2003, ApJ, 586, 419
Kalemci, E., Tomsick, J. A., Rothschild, R. E., Pottschmidt, K., & Kaaret, P. 2004a, ApJ, 603, 231
Kalemci, E., et al. 2004b, ApJ, submitted (astro-ph/0409092)
Klein-Wolt, M., Fender, R. P., Pooley, G. G., Belloni, T., Migliari, S., Morgan, E. H., & van der Klis, M. 2002, MNRAS, 331, 745
Levine, A. M., Bradt, H., Cui, W., Jernigan, J. G., Morgan, E. H., Remillard, R., Shirey, R. E., & Smith, D. A. 1996, ApJ, 469, L33
Maccarone, T. J. 2002, MNRAS, 336, 1371
———. 2003, A&A, 409, 697
Makishima, K., Maejima, Y., Mitsuda, K., Bradt, H. V., Remillard, R. A., Tuohy, I. R., Hoshi, R., & Nakagawa, M. 1986, ApJ, 308, 635
Markoff, S., Falcke, H., & Fender, R. 2001, A&A, 372, L25
Markoff, S., & Nowak, M. 2004, ApJ, 609, 972
Markoff, S., Nowak, M., Corbel, S., Fender, R., & Falcke, H. 2003, A&A, 397, 645
Markwardt, C. 2001, Ap&SS Suppl., 276, 209
Markwardt, C., Swank, J., & Smith, E. 2001, IAU Circ. 7707
McClintock, J. E., & Remillard, R. A. 2004, in Compact Stellar X-Ray Sources, ed. W. H. G. Lewin & M. van der Klis (Cambridge: Cambridge Univ. Press), in press
Meier, D., Koide, S., & Uchida, Y. 2001, Science, 291, 84
Merloni, A., Heinz, S., & di Matteo, T. 2003, MNRAS, 345, 1057
Migliari, S., Fender, R. P., Rupen, M., Wachter, S., Jonker, P. G., Homan, J., & van der Klis, M. 2004, MNRAS, 351, 186
Miller, J. M., et al. 2001, ApJ, 563, 928
———. 2002, ApJ, 570, L69
———. 2004, ApJ, 601, 450
Mirabel, I. F., & Rodríguez, L. F. 1994, Nature, 371, 46
Orosz, J. A., McClintock, J. E., Remillard, R. A., & Corbel, S. 2004, ApJ, 616, 376
Reig, P., Belloni, T., & van der Klis, M. 2003, A&A, 412, 229
Remillard, R. 2001, IAU Circ. 7707
Revnivtsev, M., & Sunyaev, R. 2001, IAU Circ. 7715
Rodriguez, J., Corbel, S., Kalemci, E., Tomsick, J. A., & Tagger, M. 2004, ApJ, 612, 1018
Rodriguez, J., Corbel, S., & Tomsick, J. A. 2003, ApJ, 595, 1032
Rossi, S., Homan, J., Miller, J. M., & Belloni, T. 2004, in The Restless High-Energy Universe, ed. E. P. J. van den Heuvel, J. J. M. in 't Zand, & R. A. M. J. Wijers (Amsterdam: North-Holland) (astro-ph/0309129)
Sanchez-Fernandez, C., Zurita, C., Casares, J., Castro-Tirado, A. J., Bond, I., Brandt, S., & Lund, N. 2002, IAU Circ. 7989
Sault R. J., & Killeen N. E. B. 1998, The Miriad User's Guide (Sydney: Australia Telescope National Facility)
Stirling, A. M., Spencer, R. E., de la Force, C. J., Garrett, M. A., Fender, R. P., & Ogley, R. N. 2001, MNRAS, 327, 1273
Tigelaar, S. P., Fender, R. P., Tilamus, R. P. J., Gallo, E., & Pooley, G. 2004, MNRAS, 352, 1015
Tomsick, J. A., Corbel, S., Fender, R., Miller, J. M., Orosz, J. A., Tzioumis, T., Wijnands, R., & Kaaret, P. 2003a, ApJ, 582, 933
Tomsick, J. A., Corbel, S., & Kaaret, P. 2001, ApJ, 563, 229
Tomsick, J. A., Kalemci, E., Corbel, S., & Kaaret, P. 2003b, ApJ, 592, 1100
Tomsick, J. A., Kalemci, E., & Kaaret, P. 2004, ApJ, 601, 439
Wijnands, R., Miller, J. M., & Lewin, W. H. G. 2001, IAU Circ. 7715